

Role of Microbiological and Geochemical Heterogeneity in the Fate and Transport of Nitrogen through the Vadose Zone

BARD project IS-4356-10

Alex Furman¹, Thomas Harter², Noam Weisbrod³, Kate Scow², Sanjai Parikh², Avi Shaviv¹, Fungai Mukome², Radomir Schmidt², Hanna Ouaknin¹, and Mor Shachar³.

1. Civil and Environmental Engineering, Technion, Israel
2. Land, Air, and Water Resources, University of California – Davis, USA
3. Environmental Hydrology and Microbiology, Ben Gurion University, Israel

Executive Summary

The main goal of this project was to study the role of heterogeneity on the biochemical activities in soil, focusing on the nitrogen cycle. Despite decades of nitrogen research the processes are only generally understood with respect to the spatial heterogeneity. We hypothesize that the local physical heterogeneity, at various scales, create local conditions that may be superior for certain biochemical activities. Specifically, we focused on soil microaggregates and distinct interfaces, where most of the work conducted by the American team was conducted in field conditions, while the Israeli team focused on synthetic, artificially created interfaces at the lab scale.

Soil microaggregates have been implicated as the primary factor for the stabilization of soil carbon in agricultural soils. We hypothesize activities that have an effect on soil microaggregates, such as long term farming management systems, have a considerable effect on soil C and N dynamics. Soils from plots under organic and conventional farming system for over 20 years were collected from the Long Term Agricultural Research Station (LTRAS) in Davis, CA. Baseline soil chemical (pH, NH₄, NO₃), and physical (particle size and bulk density) characteristics were determined. Water-stable aggregates of the soils and were isolated and measured for total C (TC), and total N (TN); total inorganic C (TIC) and total inorganic N (TIN) after hypochlorite removal of organic matter; and total organic C (TOC) and total organic N (TON) by difference. Microbial community in the microaggregates was analyzed by quantitative PCR (qPCR) for total bacteria and archaea, bacterial and archaeal nitrifiers via the conserved *amoA* genes and bacterial denitrifiers via the conserved *nirK*, *nirS* and *nosZ* genes. Organic matter composition was determined via subtractive diffuse reflectance Fourier transformed infrared spectroscopy (DRIFTS). Sub samples of the soils from the two farming systems were also used in laboratory microcosms to investigate the weekly

effect of added labeled ^{15}N fertilizer on soil aggregate distribution, microbial population dynamics, and microaggregate C and N dynamics and composition over a period of 28 days. The samples were subjected to the previous analyses. Results show comparatively higher TC, TOC, TN, and TON in the microaggregates from the organic plots. FTIR analysis showed different organic matter composition between the microaggregates of the two farming systems. The addition of the urea fertilizer resulted in increased differences between the TC and TN of the two treatments and also resulted in changes in the microaggregate organic matter composition.

Soil textural interfaces create, under flow conditions, a variety of unique local conditions such as high saturation with high availability of oxygen and alike. Biochemical activity is often controlled by oxygen and water (and primarily the transition from nitrifying to denitrifying conditions). Specifically for enhanced nitrification, high levels of both water and oxygen are desired – hence such conditions are favorable and the immediate vicinity of textural interfaces may act as local hot-spots for certain biochemical activity. In this project we investigated, numerically and experimentally, the microbial activity and the microbial ecology around such interfaces. For that purpose we designed a Hele-Shaw flow chamber that allows packing different soils separated by very sharp interfaces, and continuously monitor and sample soil state over several periods. The unique design of the system allows conducting the experiment with minimal invasion of the study domain for the routine monitoring or for extracting soil samples. Our numerical models, that consider water flow (Darcy-Richards'), solute transport (advection-dispersion) and oxygen limited biochemical activity support our hypothesis. While our experiments do continue beyond the official termination of the project, and model calibration was not yet fully conducted, we were able to observe unique microbial (genetic) signature of the microbial population at interfaces vicinity, compared to the population in the same soil far from the interfaces. We also were able to measure different redox conditions at various locations with respect to distance from interfaces.

Tying the above results with those of the field work, we suggest that local interfaces or aggregates (considered in that respect as a local porous media of fine material being in close proximity to more aerated porous media) are acting as hot-spots to various soil biochemical activities and should be given the appropriate consideration when trying to understand the spatial (and likely temporal, although that was not studied here) aspects of nitrification-denitrification.

The project included also some peripheral projects related to instrumentation and to heat transport and the way it affects soil biological phase. These are all reported in more details in the main body of the report or as appendix.

Suggested citation: Alex Furman, Thomas Harter, Noam Weisbrod, Kate Scow, Sanjai Parikh, Avi Shaviv, Fungai Mukome, Radomir Schmidt, Hanna Ouaknin, and Mor Shachar, 2014. Role of Microbiological and Geochemical Heterogeneity in the Fate and Transport of Nitrogen through the Vadose Zone. BARD (Binational Agricultural Research and Development Fund (BARD) final report project IS-4356-10.

Objectives

The objectives of this work as defined in the research proposal are:

1. to investigate the nested (sub-centimeter to centimeter to meter) scale distribution of physical, geochemical, and microbiological soil properties affecting flow and nitrogen fate and transport processes and its spatial dependency on vertical positioning in the vadose zone profile
2. to develop quantitative tools that characterize the spatial distribution and interdependence of physical, geochemical, and microbiological soil properties and nitrogen transformation processes
3. and to improve our understanding of the coupling of vadose zone flow and transport processes with biogeochemical processes to determine the effect of microbiological and geochemical heterogeneity on field scale nitrogen fate and transport

Activities of the American team

Background

Field Site

Our primary field site is the Russell Ranch Sustainable Agriculture Facility (Russell Ranch) near Davis, California. The Russell Ranch facility houses long-term research assessing the sustainability of different cropping systems by comparing system outputs and soil quality indicators. Russell Ranch is a 1500 acre tract near the UC Davis campus, which hosts the Long Term Research on Agricultural Systems (LTRAS) and Sustainable Agriculture Farming Systems (SAFS) projects. The Russell Ranch Sustainable Agriculture Facility is a unit of the Agricultural Sustainability Institute (ASI).

The facility has both long-term cropping systems comparisons and various shorter-term experiments, focused on investigating the sustainability and environmental impacts of agriculture. LTRAS is a "hundred-year" study located on the main plots at Russell Ranch. The LTRAS study began in 1993 with a uniform sudangrass crop to evaluate inherent soil differences and the original cropping systems were first planted in 1994. SAFS combined with LTRAS in 2002 to continue research on impacts of farming systems and reduced tillage practices on agronomic and soil properties, runoff and economics.

Plots were selected to obtain soils under organic and conventional farming system for over 20 years (Appendix A). Baseline soil chemical (pH, NH₄, NO₃), and physical (particle size and bulk density) characteristics were determined.

Specific objectives of the American team

1. Field: Determine the spatial variability of soil microaggregate fraction and associated biological, chemical and physical characteristics in organically and conventionally farmed soils. Determine what differences exist with depth in soils

- under same regimes as well as differences in soils under the two different farming regimes.
2. Microcosms: Determine the effect of inorganic nitrogen fertilizer on the short-term development of microaggregates (one month) in soils with a history of conventional or organic farming regime.

Hypotheses

1. Effect of farming methods on microaggregates:
 - a. more organic matter in organic treatment will lead to more stable microaggregates with higher biomass (bacteria and archaea numbers)
 - b. the relative proportions of N-cycle functional genes will be significantly different between microaggregates from conventional and organic treatments
 - c. physical distribution of aggregate sizes as well as chemical composition of microaggregates from conventional and organic treatments will show significant differences
2. Effect of inorganic nitrogen on microaggregates:
 - a. N fertilizer addition is expected to lead to increased soil microbial metabolic activity. This metabolic activity increase can have three possible outcomes on microaggregates:
 - i. microbial community utilizes easily available SOC, no net increase or decrease of microaggregates; not much increase in biomass, most SOC burned off as CO₂
 - ii. increased N allows microbes to attack SOC sequestered in microaggregates, leading to net microaggregate breakdown and soil structure degradation
 - iii. increased N and the associated increase in metabolic activity leads to increase in biomass, sequestration of C and build-up of new microaggregates

Materials and Methods

Field Sampling

Field site analysis focused on organic and conventional tomato plots at Russell Ranch. The chosen plots spanned the breadth of the facility from the most clayey to the most sandy soils (Figure A-1). Samples were obtained at 0-15, 15-30 and 30-60 cm below-ground-surface depths. Twelve semi-random samples from each depth for each plot were compiled, homogenized, and stored at -20°C before further sub-sampling and analysis.

Microaggregate Isolation

The microaggregate soil fraction (53-250 μm) is considered most important for microbial activity and generally includes high concentrations of organic carbon and very active microbial biomass. Each homogenized depth sample from each plot was therefore subjected to the microaggregate isolation protocol developed by Professor Johan Six at UC Davis. Briefly, microaggregate isolation utilized a wash/agitation/disruption step through a 250 μm screen before collection of particles on a 53 μm screen. The microaggregates were washed, then centrifuged to reduce water content and freeze dried in preparation for analysis. The silt/clay (< 53 μm) and macroaggregate (>250 μm) fractions were collected and oven dried to determine the percentage composition of each fraction in the soil.

Molecular Analysis

DNA was extracted from all microaggregate samples and analyzed by quantitative polymerase chain reaction (qPCR) assays for total bacteria and archaea (16S rRNA gene), archaeal and bacterial nitrification (AOA and AOB, respectively), and denitrification genes (nirK, nirS and nosZ). The position of the above functional genes in the nitrification and denitrification pathways is illustrated in Figure B1. Overall, the molecular analysis provided a significant insight into the microbial community composition at Russell Ranch as well as a benchmark for third year BARD project experiments (Appendix B).

Chemical Analysis

In the laboratory, the soils were sub-sampled and field moist samples used for analysis of soil moisture content. The remainder of the soil was air dried then passed through a 2 mm sieve prior to grinding and chemical analysis. The soil was analyzed for total C and N with a C/N Analyzer (ECS 4010 Costech Analyzer); pH; extractable DOC (dissolved organic carbon); $\text{NH}_4\text{-N}$ (ammonium); and $\text{NO}_3\text{-N}$ (nitrate) (Appendix C).

A small subsample of the microaggregate soil fraction was removed for organic matter composition determination using ATR-FTIR (attenuated Fourier transform infrared) spectroscopy. Collected spectra of unprocessed and treated (organic matter removed with sodium hypochlorite- pH 9.5) were subtracted to determine changes in the organic matter composition of the microaggregate fractions as a function of time.

After determining differences in the soils from the two farming systems, composite samples were collected to investigate the microbial, chemical and structural response of these differently managed soils to inorganic nitrogen addition.

Soil Microcosm Set-up

Soils – conventional and organic tomato plots sampled, composited and homogenized as described above. Approximately 30 g of homogenized soils were distributed to glass microcosm jars according to the scheme shown in Table 1. Moisture was adjusted to

50% water holding capacity, followed by a 10 day rest period before addition of labeled ^{15}N nitrogen fertilizer (urea). Based on a theoretical 100 lb N/acre fertilizer application, half the microcosms received 91.3 mg urea/kg soil.

Soil microcosm analysis

Gas efflux of N_2O and CO_2 was sampled daily for one week after the addition of urea (T=0), then weekly (Appendix D). Microcosm sets were sacrificed at T=0, then at the end of week 1, 2, 3 and 4. Microaggregates were isolated as above and analyzed by qPCR assays for total bacteria and archaea (16S rRNA gene), archaeal and bacterial nitrification (AOA and AOB, respectively), and denitrification genes (nirK, nirS and nosZ). Further chemical analysis included TC, TN, TIC, TIN, TOC and TON, and FTIR DRIFTS for functional group composition. The results from these analyses are presented in Appendix D.

Personnel

Israel Herrera <igherrera@ucdavis.edu>

Israel is the facility manager at Russell Ranch. Israel has managed the crop production and field maintenance, as well as contributing to every aspect of Russell Ranch, for 14 years.

Fungai Mukome <fmukome@ucdavis.edu>

Fungai is a postdoctoral researcher in the lab of Dr Sanjai Parikh. Fungai is an environmental chemist and has been investigating the chemistry and stability of biochar, an emergent soil amendment. He brings over 10 years of experience in soil chemical and physical analysis.

Radomir Schmidt <radschmidt@ucdavis.edu>

Radomir is a postdoctoral researcher in the lab of Dr Kate Scow. Radomir is a microbiologist who has been working on various molecular aspects of soil microbiology, from bioremediation to agricultural soil services, for the last 6 years.

Emma Torbert <eetorbert@ucdavis.edu>

Emma is a post-graduate fellow working for the Agricultural Sustainability Institute at Russell Ranch. She is working on the Russell Ranch database, web site, publications and outreach.

Jamie Yates

Jamie joined the team as an undergraduate intern in the fall of 2012. She worked on the project from 2012 to spring 2014 in the lab of Dr Kate Scow.

Laura Emberson

Laura joined the team as an undergraduate assistant in the spring of 2013 to summer of 2013 in the lab of Dr Sanjai Parikh.

Martha Sayre

Martha joined the team as an undergraduate assistant in the fall of 2013 to spring of 2014 in the lab of Dr Sanjai Parikh.

Conclusions

- Test of field soils have shown that organic farming practices lead to higher microaggregate proportion of total soils, and these microaggregates contain significantly higher numbers of bacteria and archaea, as well as specific nitrifier and denitrifier numbers.
- The relative abundances of various microbial functional groups were similar between the two soil treatments, with the exception of nosZ genes as proportion of total denitrifiers, which was significantly higher in organic soils. Organic soils have been reported as producing higher N₂O efflux than similar conventional soils in the past, so this result was not expected, but could reflect the higher substrate turnover rates in organically farmed soils.
- The microaggregates in the organic soils had more oxygen rich (carboxyl groups and esters) and aliphatic functional groups. After incubation with urea, a greater change in microaggregate functional group composition was observed in the organic soils.
- The addition of urea to microcosms trended to an increase in total microaggregates over a period of 28 days in organic soils, while no increase in microaggregates resulted in conventional soils. These results were both in contrast to the control soils with no urea addition, that both trended to a somewhat lesser increase than the organic soil microaggregates.
- The above result suggests that in organic soils N fertilizer addition tends to promote microcosm creation in the short term, while in conventional soils it may tend to lead to microaggregate destruction as the addition of N may lead to degradation of stored C.

Activities of the Israeli team

Specific objectives of the Israeli team

1. To design and construct a flow chamber that will allow running long term (several months) monitoring of dynamic biochemical activity at minimal invasion and destruction
2. To conduct various 3-month experiments in the flow chamber with differing soil layering and interfaces
3. To build and calibrate a numerical flow and transport reactive model based on the experimental data
4. Investigate biological and chemical variability in field conditions

The tragic Mt Carmel fire that happened close to the beginning time of the project made us shift the student that was working on the last objective, and instead of working on soil heterogeneity we asked her to address a new objective:

5. To study the influence of fire on soil microbial activity

Construction of a Hele-Shaw cell

The main focus of the Technion team, other than some preliminary study of research soil and their properties, was the constructions of a Hele-Shaw cell that will serve as a major tool to investigate the role of interfaces under ideal conditions. The cell (see Appendix) is made of Plexiglas, with dimensions of (roughly) 50x50x10 cm. In one wall of the cell about 900 sampling ports (8 mm inner diameter) were opened, each with a matching Plexiglas screw. About ¼ of these screws have a small hole (2.9 mm) inside for a matching rhyzon (for soil water extraction). The other wall of the cell has 18 3-rod TDR electrodes (10 cm length) embedded in the Plexiglas wall (see later in appendix calibration of these probes), and 16 ports for tensiometers and Redox probes. Wicks were constructed in the lower part of the cell to allow below-saturation lower boundary condition. At this point the cell is undergoing preliminary testing and calibration of the different instruments (including TDRs, self-made 6 mm tensiometers, rhyzons (Eijelkamp), Redox probes (Ecotech), and watering system. Several pictures of the cell in various stages are presented in Appendix.

Several technical difficulties caused delays in the operation of the cell, but it is now nearing the end of the first experiment in which the cell is constructed with three layers of relatively sandy soils, with the coarser soil at the center. Treated wastewater is used for daily irrigation and the various parameters are tracked automatically or manually during several months. Samples for microbial analysis are collected and frozen for now. Results of some of the other parameters are shown in appendix.

Wall embedded TDR probe

A wall-embedded TDR probe is primarily considered to reduce the equipment effects on the flow and microbial processes in the soil, and to reduce to minimum the instruments embedded “in” the Hele-Shaw cell to avoid damage to sensors while sampling the soil. The idea is not new although (to the best of our knowledge) was not yet practiced using regular TDR probes. A preliminary study (see appendix) showed an almost linear relation between the measured water content (and dielectric constant) and the real one, which is generally matching the theory, considering the dielectric constant of Plexiglas).

Layered soil experiments

Sample results for water content, redox potential, nitrate and ammonium concentration and matric potential are all given in appendix. We present here only preliminary analysis of the genetic signature of the different sampling locations. Most interesting is to see the

difference, not dramatic yet existent, between the upper and lower parts of the same soil (sand in this case, sandwiched between two red sandy loam layers).

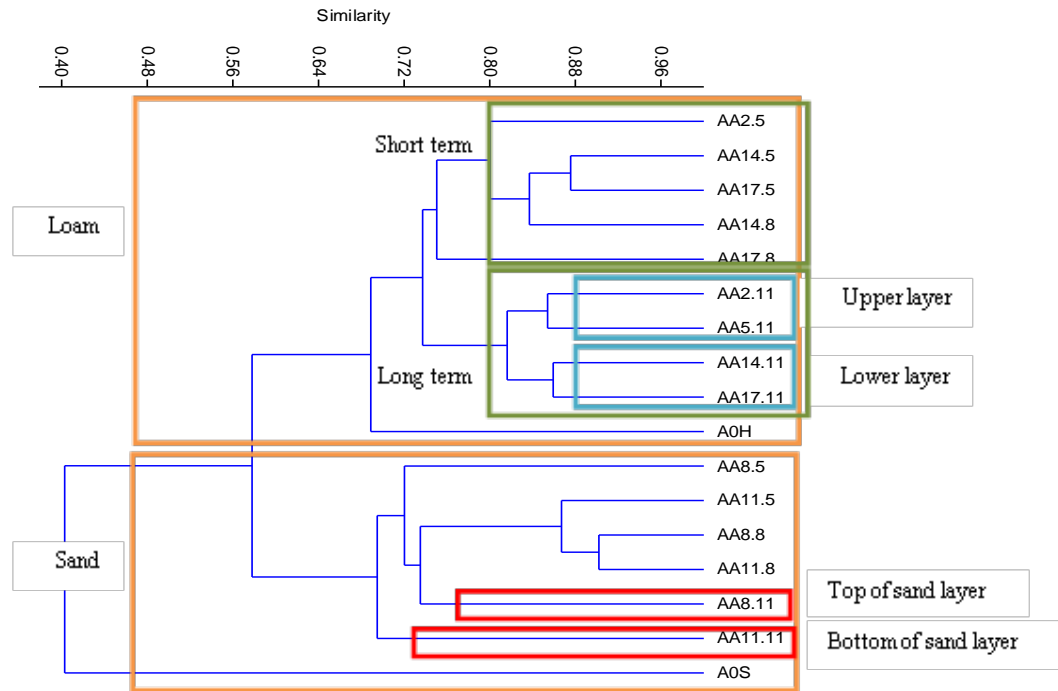


Figure 1: similarity analysis of microbial groups at different spatial locations

Numerical simulations

We have constructed, under COMSOL multiphysics framework, a flow and transport model. The model considers Richards' equation for flow

$$(1) \quad C_m \cdot \frac{\partial h}{\partial t} = \frac{\partial}{\partial z} \left(K(h) \left(\frac{\partial h}{\partial z} + 1 \right) \right)$$

The model is actually two dimensional but the horizontal dimension is uniform. In (1) the van Genuchten - Mualem parameterization is used and will not be detailed here. Solute transport is modeled for both nitrate and ammonium using the advection-dispersion equation with a sink terms for the nitrification and denitrification

$$(2) \quad R \frac{\partial (\theta c_{NH_4^+})}{\partial t} = \frac{\partial}{\partial z} \left(D \frac{\partial \theta}{\partial z} - qc_{NH_4^+} \right) - S_{nit}$$

$$(3) \quad \frac{\partial (\theta c_{NO_3^-})}{\partial t} = \frac{\partial}{\partial z} \left(D \frac{\partial \theta}{\partial z} - qc_{NO_3^-} \right) + S_{nit} - S_{den}$$

With the nitrification and denitrification modeled by

$$(4) \quad S_{nit} = r_{max}^{nit} X_1 \left[\frac{k_{b1}}{k_{b1} + X_1} \right] \left[\frac{C_{NH_4-N}}{k_{C_{NH_4-N}} + C_{NH_4-N}} \right] \left[\frac{C_{O_2}}{k_{O_2} + C_{O_2}} \right]$$

$$(5) \quad S_{den} = r_{max}^{den} X_3 \left[\frac{k_{b3}}{k_{b3} + X_3} \right] \left[\frac{C_{NO_3-N}}{k_{C_{NO_3-N}} + C_{NO_3-N}} \right] \left[\frac{k_{bO_2}}{k_{bO_2} + C_{O_2}} \right]$$

And oxygen transport, dissolved and gas

$$(6) \quad \frac{\partial}{\partial t}(\theta O_2) = \frac{\partial}{\partial z} \left(D \frac{\partial(\theta O_2)}{\partial z} - q O_2 \right) - \Gamma - r_1 y_{O_2/NH_4}$$

$$(7) \quad \frac{\partial(\theta_a O_{2,gas})}{\partial t} = \frac{\partial}{\partial z} \left(\theta_a D_0 \tau \frac{\partial O_{2,gas}}{\partial z} \right) + \Gamma$$

Naturally it is too difficult to represent all simulation results. We focus here at two points related to a) the role of the interfaces, and b) the use of Monod kinetics versus first order kinetics considering oxygen concentrations. Figure 2 presents the spatial distribution of the difference nitrogen species under homogeneous and layered conditions.

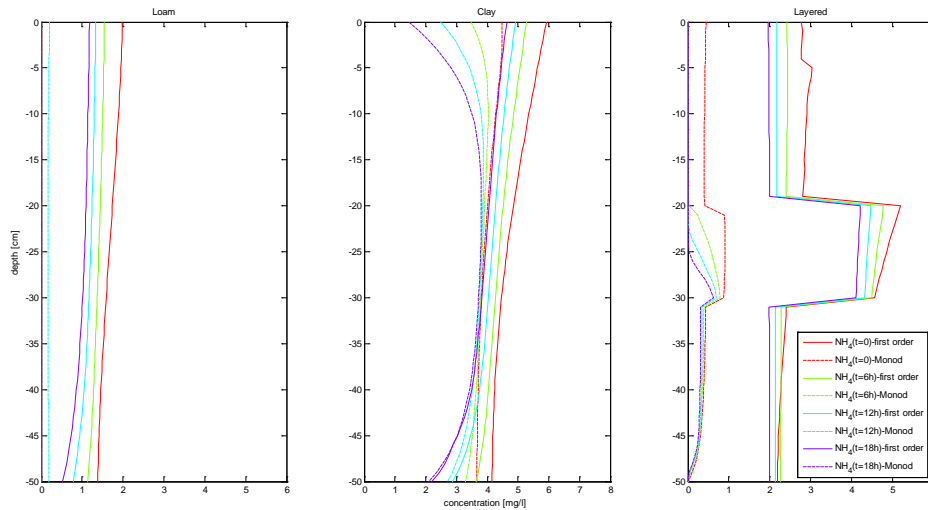


Figure 2: ammonium concentration for homogeneous red-sandy loam (left), clay (center), and layered case (right, clay sandwiched between red-sandy loam layers) comparing first order and Monod kinetics

Note specifically the high nitrification rates in the homogeneous clay under first order, and its significant reduction under Monod kinetics. Also note the reduction in nitrification in the clay layer (higher concentration), but consider the spatial variability within that layer (20-30 cm) under Monod kinetics. Further results are brought in appendix.

Soil microbiology under fire

Wildfire affects forest ecosystems. The overall effects are complex, ranging from the removal of above-ground biomass to changing physical, chemical, and microbial

processes of the soil. The flames heat the soil and remove the vegetation cover. Without the above-ground cover, the soil has larger exposure to a wide range of extreme temperatures. In general, below-surface temperatures will rise relatively slowly due to the fact that dry soil is a very good insulator. The temperature distribution (heat wave) into the soil depth is affected by several factors, including the fire intensity and its duration, soil water content, and the soil properties.

The main goal of this research is to quantify the heat distribution into soil profile due to wildfire and to examine the post-fire changes in soils' physico - chemical properties. For further details and experimental setup, field, lab, and numerical results see appendix.

Personnel

1. Hanna Ouaknin hana@tx.technion.ac.il
Hanna is a student at the Technion. She started as a master student and is now in transition to direct PhD program. Her major role in the project is the construction and operation of the Hele-Shaw cell.
2. Mor Shachar mori.shachar@gmail.com
Mor is a master student at BGU. Her major role in the project is the investigation of "microbiology under fire"
3. Yael Meyouhas
Yael is an undergraduate student working in the project, primarily helping Hanna. We hope to recruit her as a master student that will take responsibility over the field sampling activity.
4. Efrat Kohen
Efrat is an undergraduate student that replaced Yael (graduated)
5. Naomi Pardo
Naomi is an undergraduate student that replaced Efrat (graduated)

Meetings

Prior to the beginning of the project Furman and Weisbrod used an unrelated visit to the US to visit the American team at UC-David (Dec. 2010). A full day of discussions served as a kick-off to the project and lead to constricting ideas for both teams. Harter, Weisbrod and Furman met and discussed progress during the last AGU meeting (December 2012). Furman is spending a sabbatical in UC-Davis in the last few months which helps tying the pieces together and will hopefully lead to joint publications.

Appendix A: Russell Ranch field site

The Russell Ranch field site consists of 72 one acre plots (Figure A1). Crops are planted on a two-year rotation schedule. Each treatment schedule has three plots distributed randomly throughout the site. Over the project, soils were collected from organic (1-2, 6-5, 8-8) and conventional (1-4, 5-5, 7-8) plots



Figure A1. Aerial view of plots at Russell Ranch showing location of sampled plots and their management system. Variability in soil clay and sand content indicated by arrow.

Sampling events took place in the spring, summer and fall of 2012; spring and fall of 2013 and spring of 2014.

Appendix B: qPCR data collected at Russell Ranch

The microaggregate fractions of soil samples from conventional crop rotation plots at Russell Ranch were analyzed for total microbial biomass as well as functional genes from nitrogen cycle pathways (Figure 3). The first step in the nitrification pathway can be performed by either bacterial or archaeal *AmoA*. The reduction of nitrite by denitrifiers can be performed either by a copper nitrite reductase (*NirK*) or by a cytochrome *cd1* nitrite reductase (*NirS*); denitrifying bacteria possess only one type of *Nir*. The final step of denitrification, the reduction of nitrous oxide to dinitrogen is carried out by *NosZ*. The abundance of *nosZ* genes in the denitrifying community is thought to be indicative of the community's denitrification efficiency.

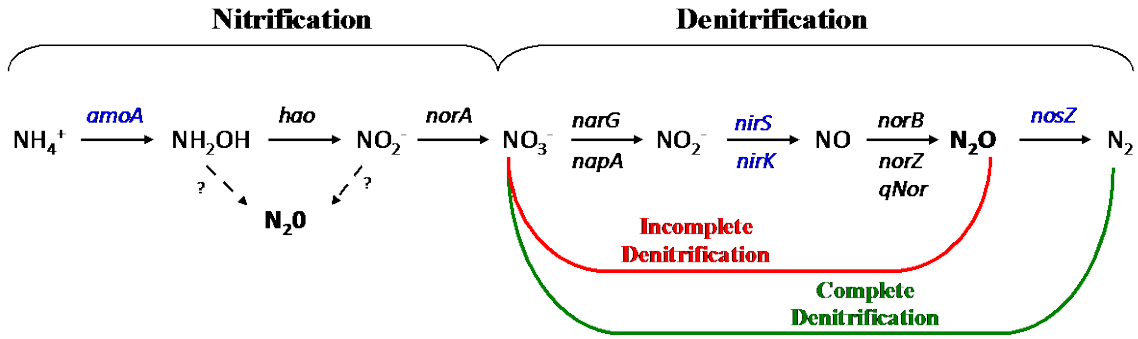


Figure B-1. Nitrification and denitrification pathways. Functional genes representing key, conserved steps in each pathway that have been assayed to date are indicated in blue.

The 16S rRNA gene numbers correlate with microbial biomass. Both total DNA extracted and microbial biomass decreased rapidly with depth in a manner consistent between plots. Similar results were observed for each sampling event.

Microaggregates

Microaggregates as percent of whole soil declined with depth (Figure B2). Organic soils contained lightly higher microaggregate numbers than conventional soils, although they were only significantly different at 15-30 cm bgs.

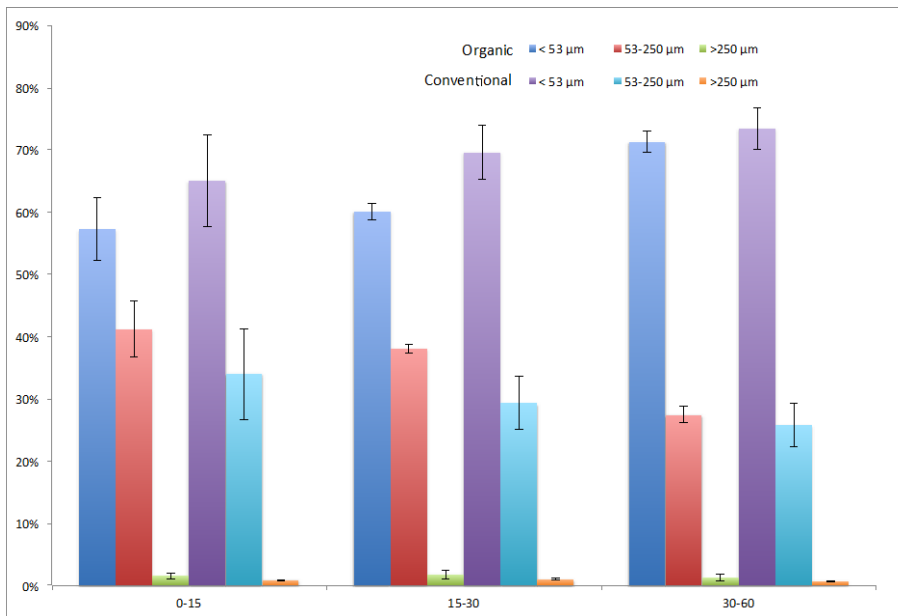


Figure B2. Proportion of silts and clays (<53 μm), microaggregates (53-250 μm) and macroaggregates (>250 μm) in organic and conventional farmed soils at Russell Ranch. Error bars of one standard deviation, n=3.

Total bacteria, archaea, AOA, AOB, nirK, nirS and nosZ genes were analyzed by qPCR (Table B1 and B2). Total microbial numbers were typically 2-5 times higher in organic than conventional soils. The percentage of archaea as function of total microbes was

only significantly different at 0-15 cm, with higher proportion of archaea at this depth (Figure B3 a)). Proportion of total nitrifiers as AOA increased with depth, but was virtually identical in both conventional and organic soils (Figure B3 b)). The proportion of the last step gene (*nosZ*) to total denitrifiers (*nirK* + *nirS*) was significantly higher at all depths in the organic soils, suggesting higher percentage of bacteria in organic soils are capable of carrying denitrification to completion (Figure B3 c))

Table B1. Total microbial and nitrifier gene numbers per gram of soil; errors 1 standard deviation (n=3).

Treatment	Plot	Depth	16S bact	16S arch	AOA	AOB
Organic	1	00-15	2.00E+10 ± 3.53E+09	9.18E+08 ± 1.28E+08	1.06E+08 ± 1.71E+07	3.58E+08 ± 5.39E+07
	2	15-30	1.96E+10 ± 5.44E+08	8.72E+08 ± 4.44E+07	1.02E+08 ± 9.85E+06	3.12E+08 ± 4.35E+07
	3	30-60	1.26E+10 ± 8.03E+08	6.72E+08 ± 4.02E+07	3.47E+07 ± 8.50E+06	1.26E+08 ± 1.93E+07
Conventional	4	00-15	1.02E+10 ± 4.01E+08	2.95E+08 ± 2.73E+07	4.51E+07 ± 7.92E+06	1.24E+08 ± 1.41E+07
	5	15-30	8.35E+09 ± 6.05E+08	4.07E+08 ± 1.07E+08	4.18E+07 ± 1.29E+07	7.87E+07 ± 1.93E+07
	6	30-60	5.56E+09 ± 4.32E+08	2.03E+08 ± 7.07E+07	2.52E+07 ± 5.17E+06	4.57E+07 ± 1.04E+07

Table B2. Total denitrifier gene numbers per gram of soil; errors of 1 standard deviation (n=3).

Treatment	Depth	<i>nirK</i>	<i>nirS</i>	<i>nosZ</i>
Organic	00-15	1.33E+07 ± 2.63E+06	2.32E+06 ± 1.19E+06	1.69E+07 ± 1.98E+06
	15-30	1.36E+07 ± 1.94E+06	1.91E+06 ± 2.07E+06	1.66E+07 ± 9.70E+05
	30-60	5.64E+06 ± 6.91E+05	3.84E+05 ± 2.00E+05	6.26E+06 ± 7.16E+05
Conventional	00-15	7.92E+06 ± 2.72E+06	1.62E+06 ± 2.40E+06	8.84E+06 ± 4.78E+05
	15-30	9.32E+06 ± 2.42E+06	1.32E+06 ± 6.69E+05	6.12E+06 ± 7.79E+05
	30-60	5.75E+06 ± 4.61E+05	1.09E+06 ± 6.09E+05	3.69E+06 ± 2.35E+05

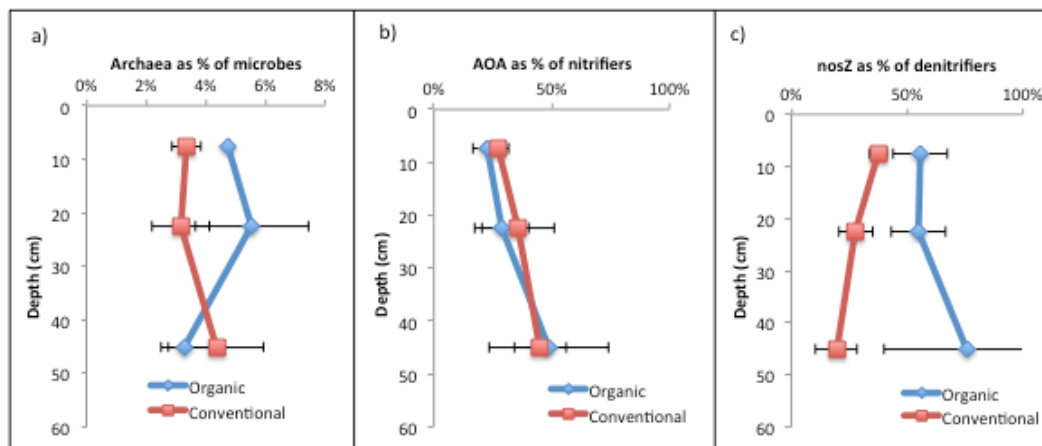


Figure B3. Prevalence of specific groups of microbes in the organic and conventional soils at three depths (0-15 cm, 15-30 cm, 30-60 cm) a) total archaea expressed as percent of all microbes (archaea + bacteria); b) total AOA as percent of all nitrifiers (AOA

+ AOB); c) total nosZ as percent of all denitrifiers (*nirK* + *nirS*). Error bars of one standard deviation (n=3).

Principal component analysis of microaggregate microbial composition (bacteria, archaea, AOA, AOB, *nirK*, *nirS*, nosZ), % microaggregates in soil and POXC showed clear separation of the soils in the 0-30 cm depth, with deeper soils showing some overlap. The variables most characteristic for the first three dimensions were: dimension 1 – treatment; dimension 2 – depth and archaea; dimension 3 – microaggregates and POXC (Figure B4 and B5).

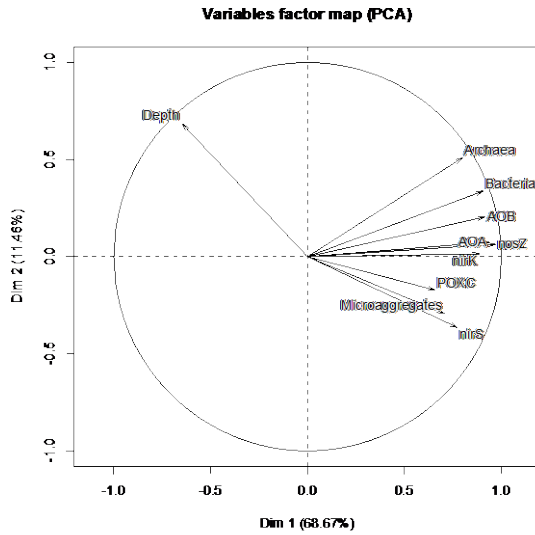


Figure B4. PCA analysis of conventional and organic tomato plot soils from Russell Ranch.

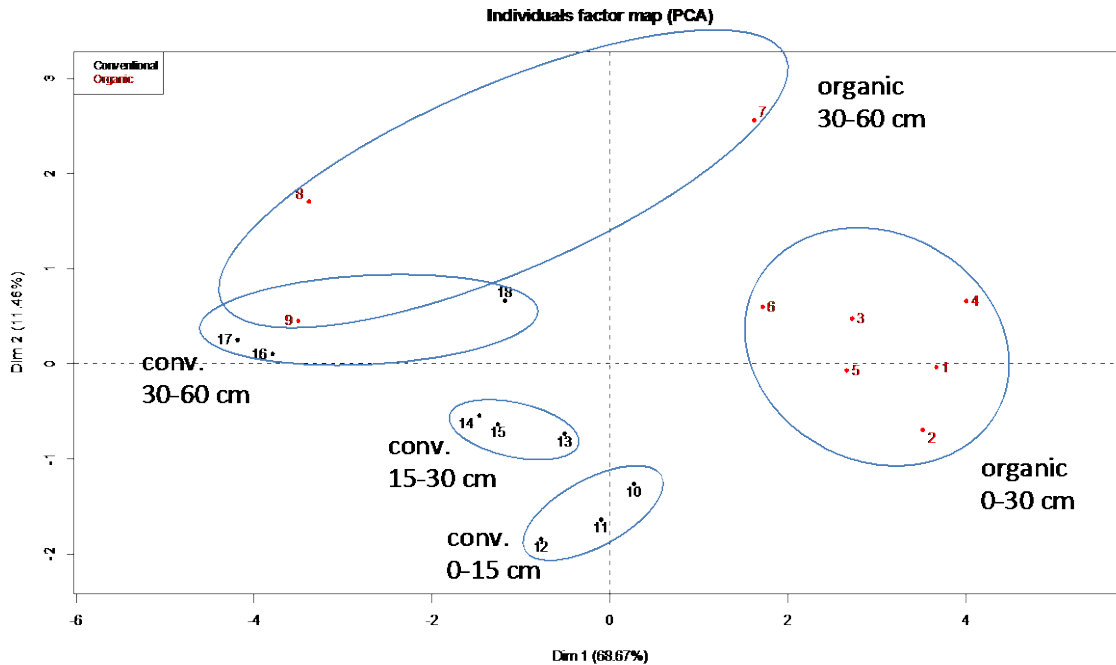


Figure B5. PCA analysis of conventional and organic tomato plot soils from Russell Ranch.

Appendix C. Physical and Chemical soil data analysis

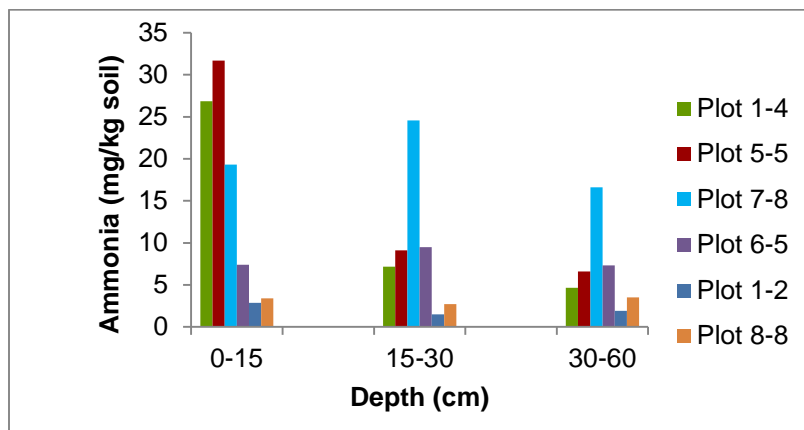


Figure C1: Ammonium concentration in soils from organic (1-2, 6-5 and 8-8) and conventional (1-4, 5-5 and 7-8) plots.

The ammonium data show a decreasing trend in ammonium with depth and consistently higher concentrations in the conventional soils.

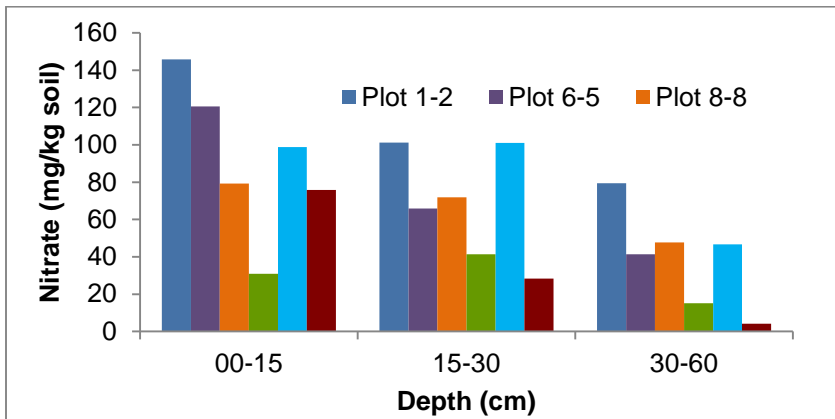


Figure C2: Nitrate concentration in soils from organic (1-2, 6-5 and 8-8) and conventional (1-4, 5-5 and 7-8) plots.

As with the ammonium, the nitrate concentration generally decreased with depth with a higher concentration in the organic soils.

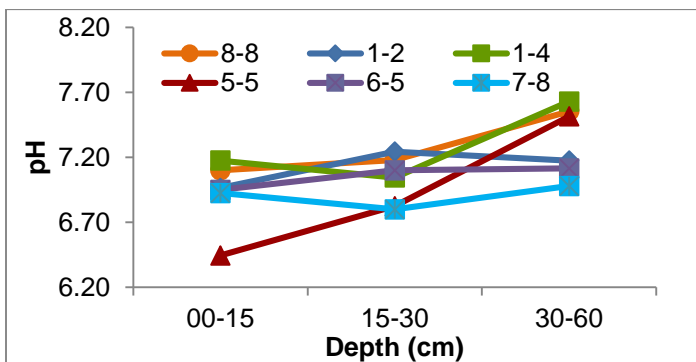


Figure C3: pH in soils from organic (1-2, 6-5 and 8-8) and conventional (1-4, 5-5 and 7-8) plots.

There was a trend of increasing pH with depth for all the plots and in addition, there was generally no difference in the pH values from the soils under the different management systems. The only exception was the upper horizon (0-15 cm) in plot 5-5 which had a much lower pH than all the other plots.

After processing the soils to attain the microaggregate (53-250 μm) fraction, further chemical analysis was performed.

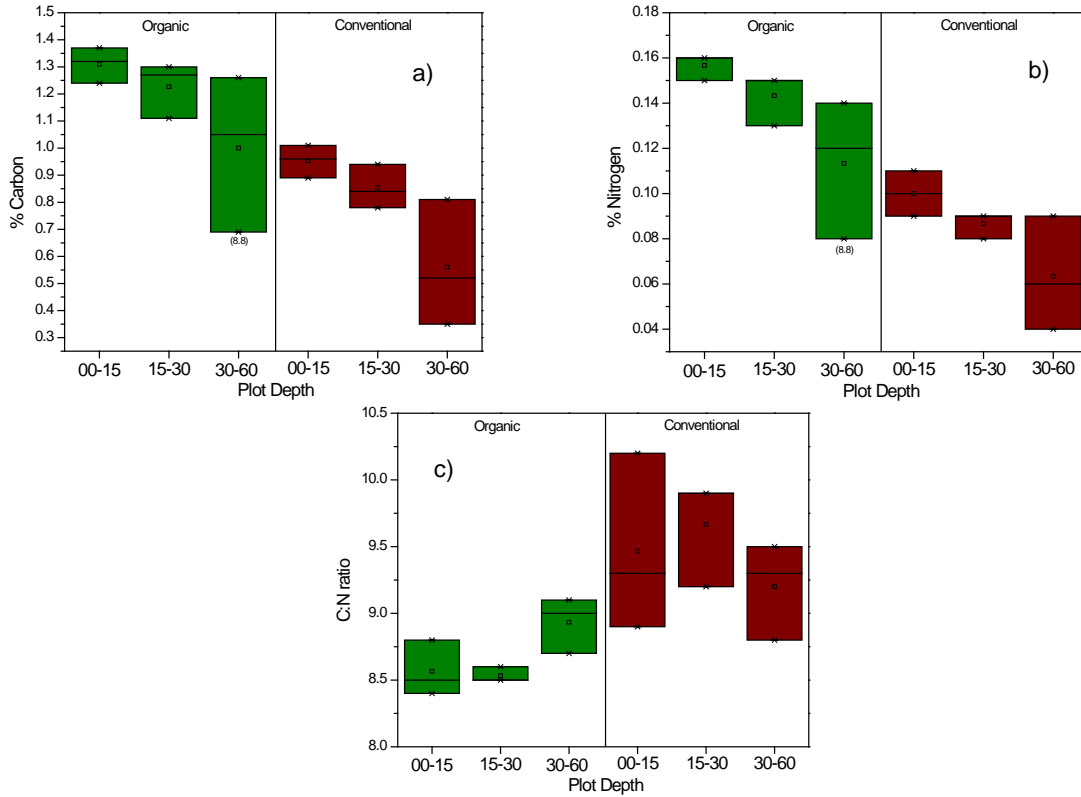


Figure C4: Plots showing the ranges in a) total carbon; b) total nitrogen; and c) C:N ratio in the microaggregates of the soils collected from the organic and conventionally managed plots.

As shown in Figure C4, both total carbon (C) and nitrogen (N) measured in the organic microaggregates was consistently higher than the conventional microaggregates and this was observed at all depths. Both properties also decreased with depth for all the plots. The plots also show that variability within the soils under the same management system increased with depth. The C:N ratios were slightly higher in the conventional microaggregates and there was also more variability in the ratios.

Appendix D: Soil microcosms

Table D1. Sample numbers for triplicate soil microcosm #1 set-up.

Week	Organic Soil Control	Organic Soil Urea	Conventional Soil Control	Conventional Soil Urea
T=0	1	16	31	46
	2	17	32	47
	3	18	33	48
T=1	4	19	34	49
	5	20	35	50
	6	21	36	51
T=2	7	22	37	52
	8	23	38	53
	9	24	39	54
T=3	10	25	40	55
	11	26	41	56
	12	27	42	57
T=4	13	28	43	58
	14	29	44	59
	15	30	45	60

Microcosms were destructively sampled immediately before the addition of urea and at the ends of weeks 1 – 4.

Gas Fluxes

CO₂

Under the conditions of the experiment, the organic control soil produced slightly more CO₂ than the conventional control soil (Fig D1). The treatments with added urea fertilizer had significantly greater emission of CO₂ compared to the controls. The organic soil emitted the greatest amount of CO₂ and the fluxes were statistically different to those from the fertilized conventional soil for the duration of the headspace gas measurements. Interestingly, by the end of the measurements, the CO₂ production for the fertilized conventional soil was consistently lower than that of the other three treatments. This is consistent with the lower total microbial population in the conventional soils.

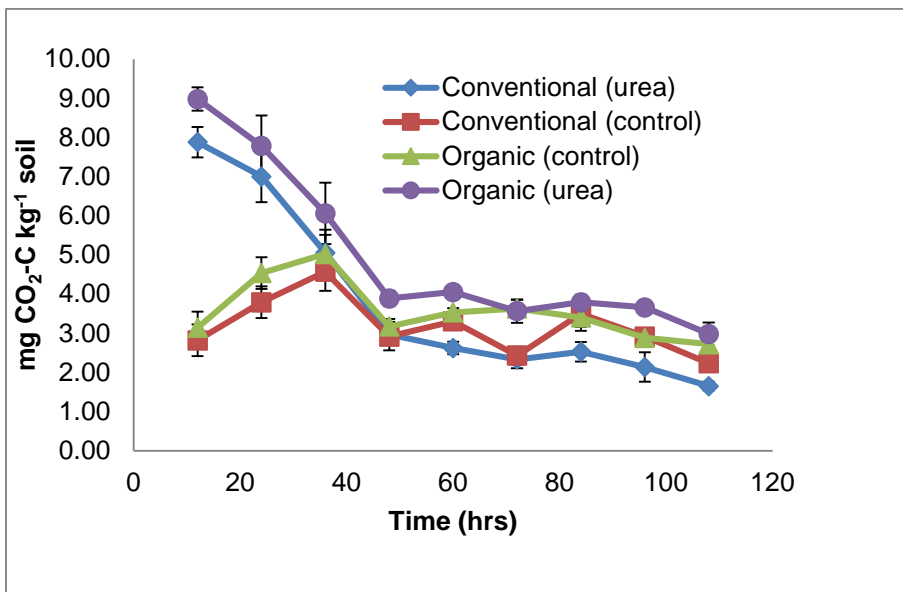


Figure D1: Graph showing the CO₂ emissions from the conventional and organic soils with and without urea fertilizer.

N₂O

As with the CO₂ emissions, the treatments with urea fertilizer consistently had greater N₂O emissions than the controls (Figure D2). Emissions from the fertilized organic soil treatments were highest throughout the measurement period. The treatments show an immediate response to the presence of the urea fertilizer and after 72 hrs, the fluxes from the fertilized organic and conventional plots are not significantly different.

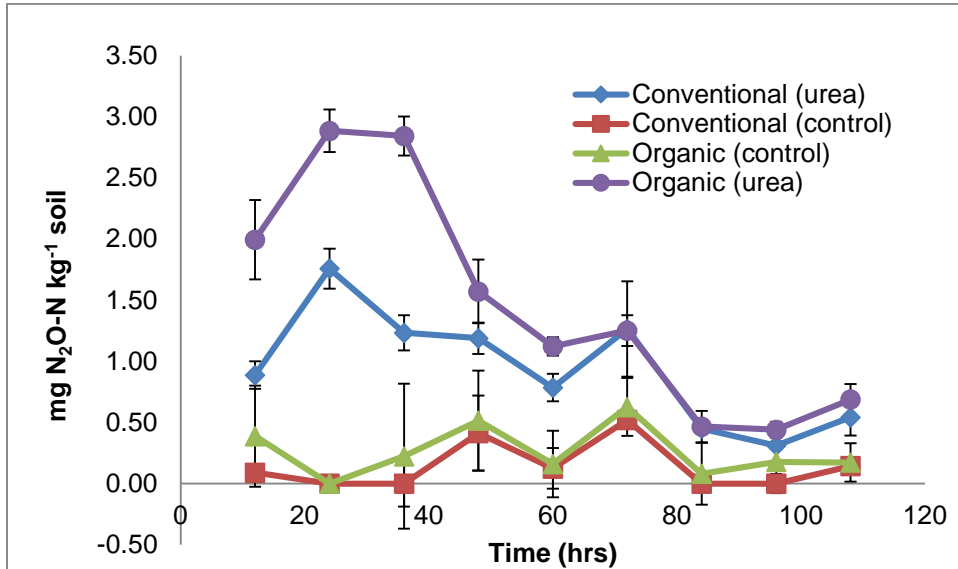


Figure D2: Graph showing the N₂O emissions from the conventional and organic soils with and without urea fertilizer.

To ensure the difference in N₂O emissions observed could be attributed to the added urea, the headspace N₂O was isotopically analyzed for the ¹⁵N contribution. As seen in Fig D3, the two soils have different potentials of transforming the added N. The organic soil had a significantly higher contribution of ¹⁵N in the emitted N₂O. The data suggest fertilizing of the organic soils with inorganic fertilizer will likely result in greater spikes in GHG emissions.

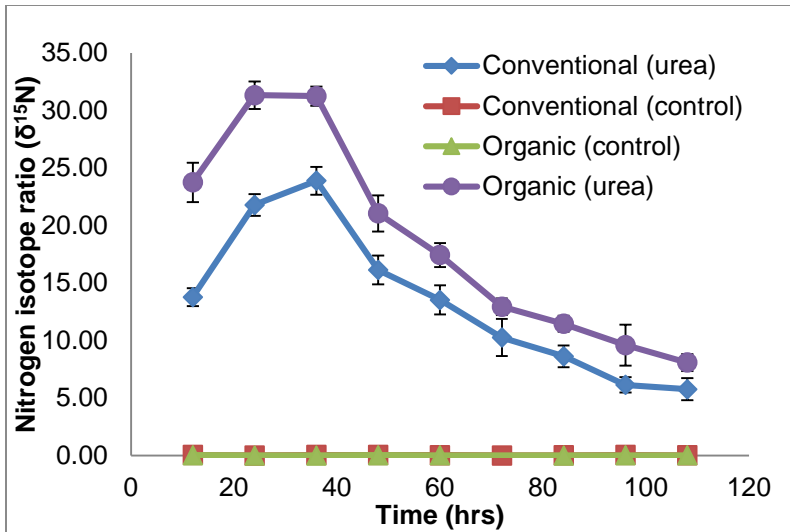


Figure D3: Graph showing the ^{15}N contribution to the emitted N_2O from the conventional and organic soils with and without labeled ^{15}N urea fertilizer.

Microaggregate Functional group composition

The FTIR spectra (Figure D4) showed the functional group composition of the soils from the two farming systems. The composition of functional groups in the two soils is similar but notably, the organic soils had a greater proportion of carboxyl groups ($\sim 1640\text{ cm}^{-1}$) and aliphatic C-H ($\sim 1420\text{ cm}^{-1}$). After the incubation, the conventional soils had a comparatively smaller change in the microaggregate functional group composition when compared to the organic soils. For the organic soils, the greatest change in composition was observed in the urea fertilized soils.

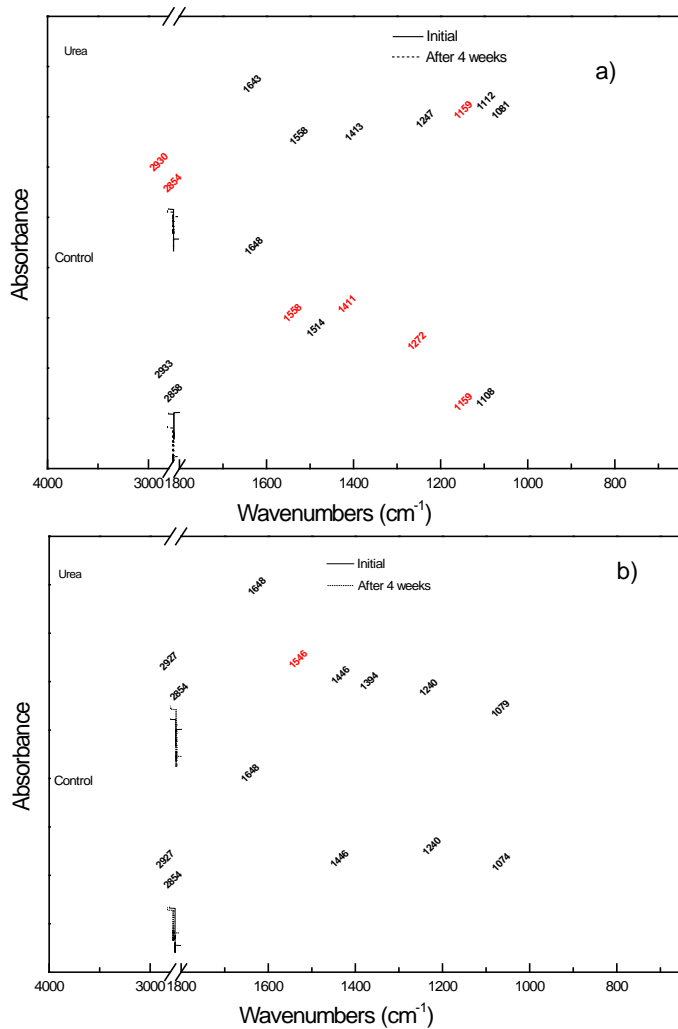


Figure D4: FTIR DRIFTS analysis of the microaggregates showed functional group composition of the a) organic and b) conventional soils before and after the incubations.

Urea fertilizer addition resulted in an increase in microaggregates in the organic soils but no change in aggregate composition was observed in the conventional soils (Table D5). Microcosms microorganism ratios were not very consistent with field samples.

Table D2. Change in microaggregate composition as percentage of whole soil in Microcosm #1 experiment; day 0-28.

	Change in microaggregate composition of whole soil (%)
Org. Control	4.2 ± 6.2
Org. Urea	7.8 ± 4.3
Conv. Control	5.4 ± 5.6
Conv. Urea	0.8 ± 4.0

All genes and microaggregate numbers showed correlation in organic control, while the addition of urea disrupted some of the apparently universal correlation in organic soil (Table D3 a) and c)). Archaea and microaggregates did not correlate to each other or to other variables in conventional treatments (Table D3 b) and d)). Conventional farming practices may lead to an imbalance in overall soil microbial community composition (archaea out of sync with other constituents), and lack of soil structure improvement (no microaggregate increase).

Table D3. Spearman pairwise correlation tables for microaggregates; microcosms #1 - a) organic control, b) conventional control, c) organic urea addition, d) conventional urea addition. P < 0.05.

a)							b)						
Org. Control	Bacteria	Archaea	AOA	AOB	nirK	nirS	Conv. Control	Bacteria	Archaea	AOA	AOB	nirK	nirS
Bacteria	1.00						Bacteria	1.00					
Archaea	0.84	1.00					Archaea		1.00				
AOA	0.78	0.83	1.00				AOA	0.91		1.00			
AOB	0.84	0.86	0.85	1.00			AOB	0.91		0.85	1.00		
nirK	0.80	0.69	0.70	0.79	1.00		nirK	0.66		0.47	0.60	1.00	
nirS	0.92	0.73	0.61	0.81	0.79	1.00	nirS	0.83		0.75	0.76	0.77	1.00
Microaggregate	0.54	0.52	0.58	0.52	0.58	0.46	Microaggregate						
c)							d)						
Org. Urea	Bacteria	Archaea	AOA	AOB	nirK	nirS	Conv. Urea	Bacteria	Archaea	AOA	AOB	nirK	nirS
Bacteria	1.00						Bacteria	1.00					
Archaea	0.69	1.00					Archaea		1.00				
AOA	0.52		1.00				AOA	0.58		1.00			
AOB	0.74	0.82		1.00			AOB	0.66			1.00		
nirK					1.00		nirK	0.85		0.72	0.70	1.00	
nirS	0.67	0.57	0.56			1.00	nirS	0.68		0.66	0.56	0.68	1.00
Microaggregate		0.54		0.60		0.52	Microaggregate						

Principal component analysis of microaggregate microbial composition (bacteria, archaea, AOA, AOB, nirK, nirS, nosZ), % microaggregates in soil and TOC, TON, TIC, TIN showed clear separation of the soils based on treatment history (organic vs conventional) and time (T = 0 and 4 vs T = 15 and 22) Figure (D5 and D6).

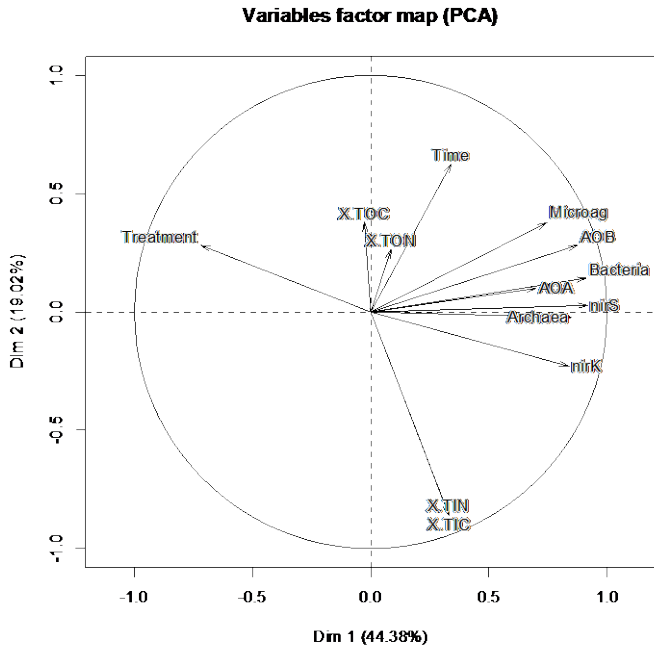


Figure D5. PCA analysis of microcosm experiment - conventional and organic tomato plot soil derived microcosms with and without urea addition. Plot parameters include qPCR numbers for bacteria, archaea, AOA, AOB, nirK, nirS, % microaggregates in soil and TOC, TON, TIC and TIN.

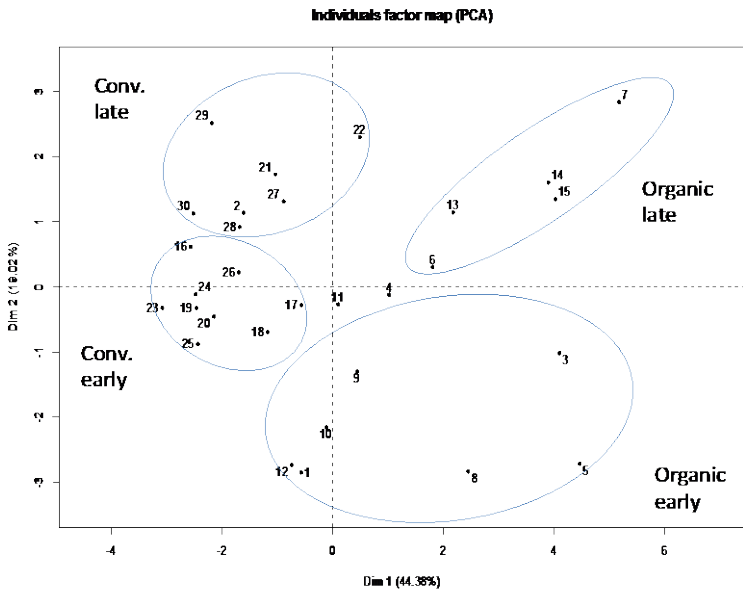


Figure D6. PCA analysis of microcosm experiment - conventional and organic tomato plot soil derived microcosms with and without urea addition. Plot parameters include

qPCR numbers for bacteria, archaea, AOA, AOB, nirK, nirS, % microaggregates in soil and TOC, TON, TIC and TIN.

Appendix E: Hele-Shaw cell experiments

As mentioned above the main working tool of the Israeli team is the Hele-Shaw flow cell that allows generation of virtual soil scenarios. The cell allows measurement and sampling across interfaces, as can be partially seen in Figure 1. We allow measurement of water content (through wall embedded TDR probes), pressure head (using self made miniature tensiometers), redox (using micro sensors by Eco-Tech, Bonn, Germany), and also liquid (using ryzhons) and solids (using close to 1000 sampling ports). Our current experiments use treated wastewater (secondary treatment) evenly distributed at soil surface in a single pulse daily. Figure 2 depicts the dynamics of the parameters measured so far. The difference in state above and below the interfaces is clearly seen, especially for water content (both interfaces) and redox (upper one). Redox phenomenon is especially interesting as in addition to daily signal a three-day cycle, that cannot be explained currently, is seen.



Figure 1: images of Hele-Shaw cell. Sampling wall (left) and TDR/tensiometer/redox wall (right)

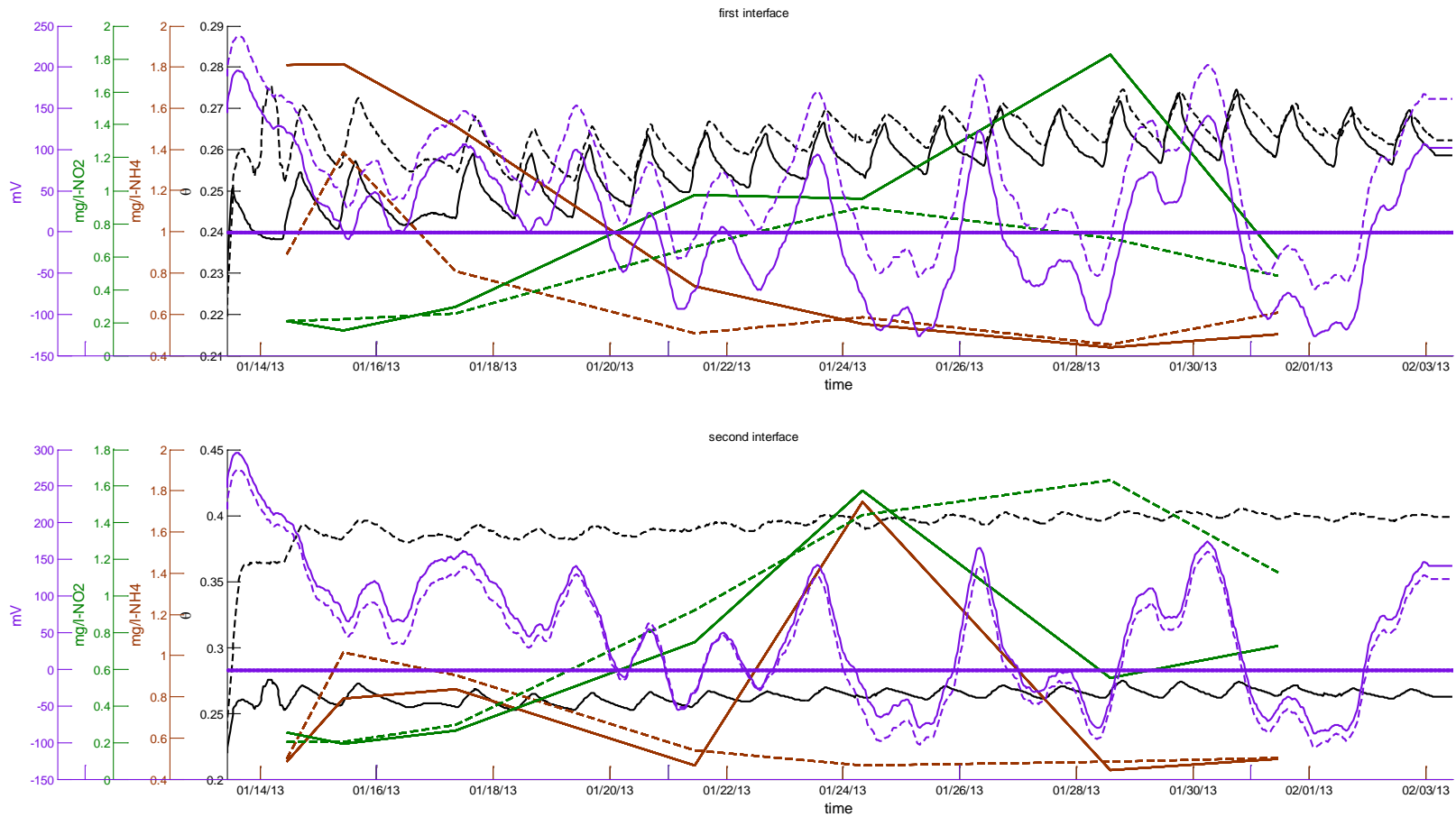


Figure 2: variation of water content (black), redox potential (purple) and nitrogen species (green and brown) for the upper and lower interfaces. Solid lines indicate values above the interface and dashed below it

Appendix F: numerical simulations

In the following we present several simulation results, most comparing either temporal variation of nitrogen (nitrate and ammonium) or spatial distribution of it after the system reached cyclic conditions (pseudo steady state)

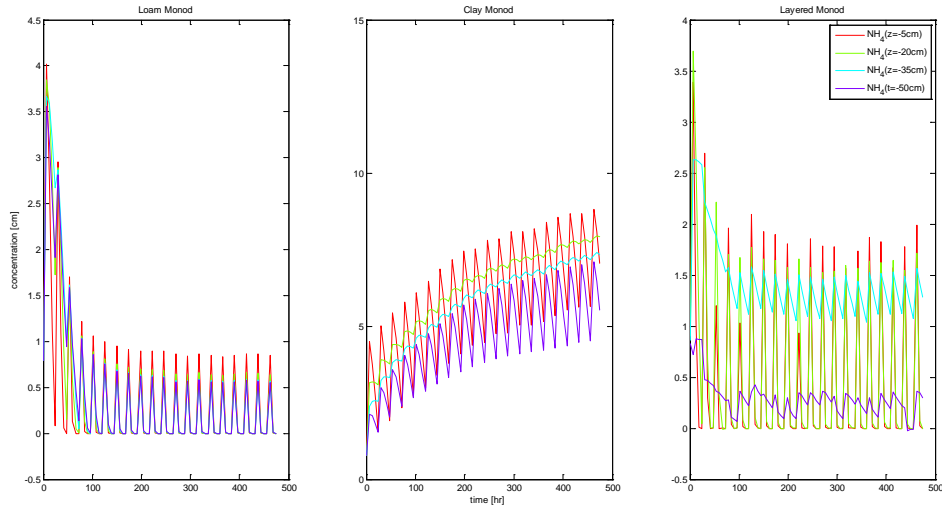


Figure 1: temporal behavior of homogeneous and layered systems

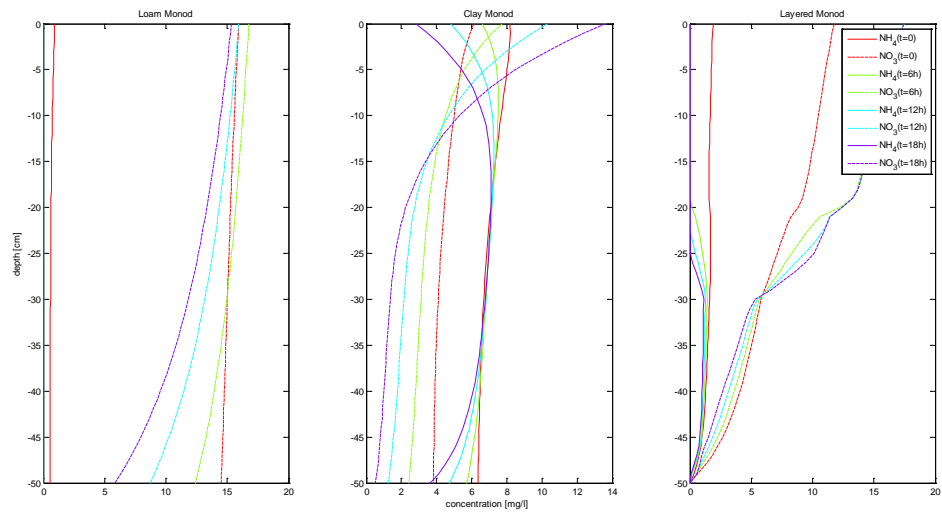


Figure 2: spatial variation of nitrate and ammonium in homogeneous and layered systems

Appendix G: Fire effects on soil physico–chemical and biological properties

Fire effects on soil physico–chemical and biological properties were examined under field and laboratory conditions. In addition, the soil’s heat and moisture transfer was simulated using numerical simulation. This report includes the achievements from the second year, and consists of three parts: a. Field sampling and lab analyses, b. Laboratory experiments, c. numerical simulation.

Field sampling and lab analyses

Soil samples from burned and unburned sites in the Carmel area were collected and analyzed to explore the fire effects on the physico-chemical and biological soil properties. For physical-chemical properties no significant changes were detected between the burned and the unburned soil samples, however the microbial abundance and diversity shows differences between the different sites and time points.

Following the fire event (December 2010) bacterial community composition had changed; the abundance reduced significantly only under the inter-shrub plots, though, the bacterial diversity was changes in both inter and under-shrub plots. Changes in the abundance of the dominate phyla were detected (Figure 2; Figure 3) - the population of Actinobacteria was decreased while the Firmicutes population was increased, the Proteobacteria maintained its relative percentage in the population.

Changes also were detected in the distribution within the dominant phyla, the Firmicutes showed spatial and temporal differences in its major classes, Bacilli and Clostridia. The Bacilli (order) - Bacillales (family) significantly increased directly after the fire event. This increase might be due to *Bacillus*’s ability to resist the environmental stresses due to spore forming nature (Pandey et al. 2011).

Three months after the fire (March 2011), the abundance in the inter-shrub was increased; the Bacillales still shows higher population in the burned site, however lower than in December 2010. The main change in the bacterial population in March 2011 is the increase in the Proteobacteria’s population, mainly in the under shrub plot.

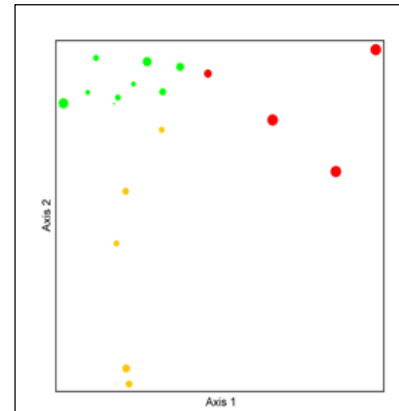


Figure 1 – two dimensional distribution of bacterial community composition. Green indicates the samples from the burned site from both time points, orange and red indicate samples from the burned sites – orange from December 2010 and red from March 2011

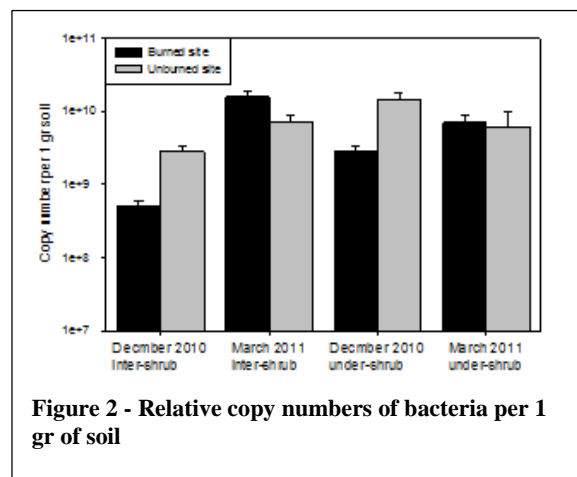


Figure 2 - Relative copy numbers of bacteria per 1 gr of soil

In contrast to changes in the bacterial community's composition in the burned sites at both time points, in the unburned sites the bacterial composition remained similar during the entire period; hence it was not affected by the change of seasons.

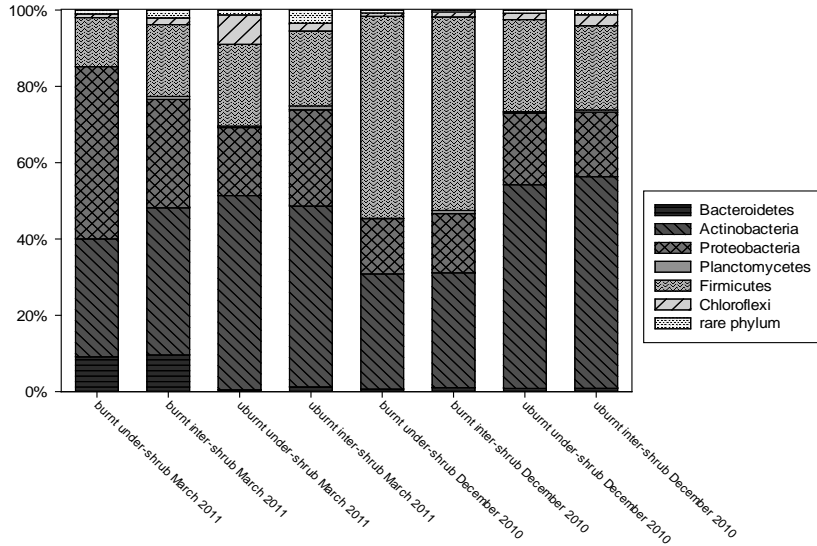


Figure 3 – phyla distribution in soil samples collected in burned and unburned sites, and inter- and under-shrub plots December 2010 and March 2011.

Laboratory experiments

Heat experiments were conducted for three different types of soil and under three different soil moisture conditions: a. dry soil b. saturated soil c. receding drying front. According to our results for the tested soils – soil type and grain size had minimal impact, therefore the distribution curves under the same moisture condition quite similar for the three soil types. Result for Eyn-Hod soil (Figure 4), shows the temperature change (Y axis) during the time (X axis) for the different depths (represent by the color of the curve).

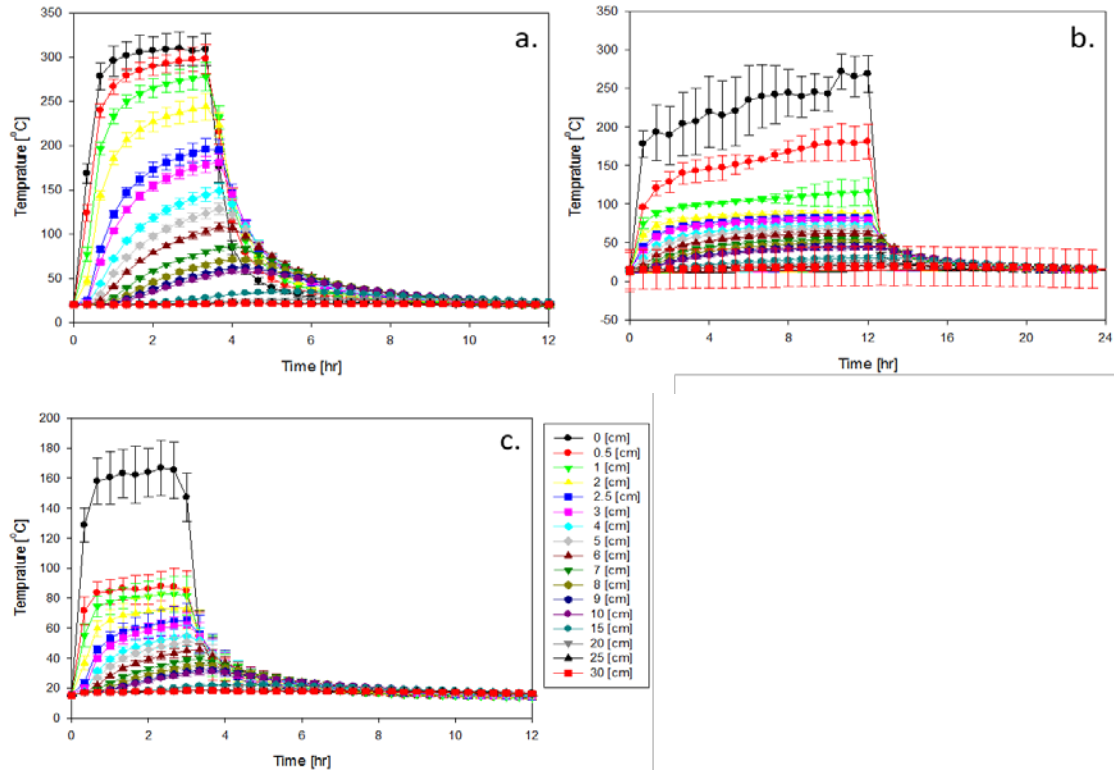


Figure 4 – heat distribution into soil depth in three water content conditions: a. dry soil; b. saturated soil (constant water level at the top); c. variable moisture conditions (saturated at the beginning with free evaporation; i.e., decreasing drying front)

Microbial abundance was analyzed for the column experiment under three moisture conditions, dry soil, receding drying front, in addition to soil at ~3% moisture mimicking the natural conditions in the field. Comparison between the gene copy number before and after heating, show that the microbial abundance was affected by the temperature and the moisture (Figure 5). Under high temperature and low moisture condition, significant changes were detected, for example under the 3% moisture the surface and 2.5cm depth significantly differed, ($p=0.004$; $p=0.003$, respectively). Under higher moisture condition, receding drying front condition, significant changes were detected in the microbial abundance before and after the heating ($p=0.05$) only in the surface which reached almost 300°C.

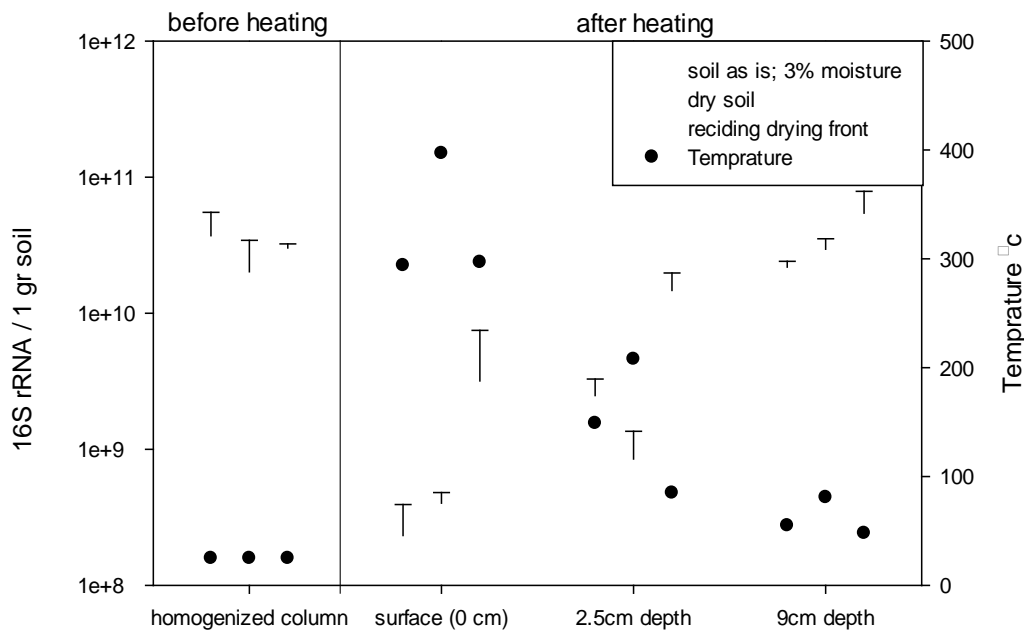


Figure 5 - microbial abundance in the column heating experiments, before and after heating for three depths (0, 2.5 and 9cm) and under three moisture conditions: 3% moisture; 0% moisture; receding drying front

Numerical simulation

Basic one-dimensional simulations describing the heat distribution into the soil depths were conducted for two steady moisture conditions: dry and saturated soil. The simulations were based on the heat transfer equation. The simulation was programmed using MATLAB software, the numerical method which was implemented in the simulation is the "The Numerical Method of Lines for Partial Differential Equations" (MOL).

In order to get high correlation between the simulation and the laboratory heat experiments two assumptions were tested: 1. Heat loss in the horizontal direction 2. Linear change of the thermal conductivity (K) with the temperature.

Figures 6 – 7 presents comparison between the results of the laboratory experiment (solid line) and the simulation (dash line) under the dry soil condition (Figure 6) and the saturated soil condition (Figure 7).

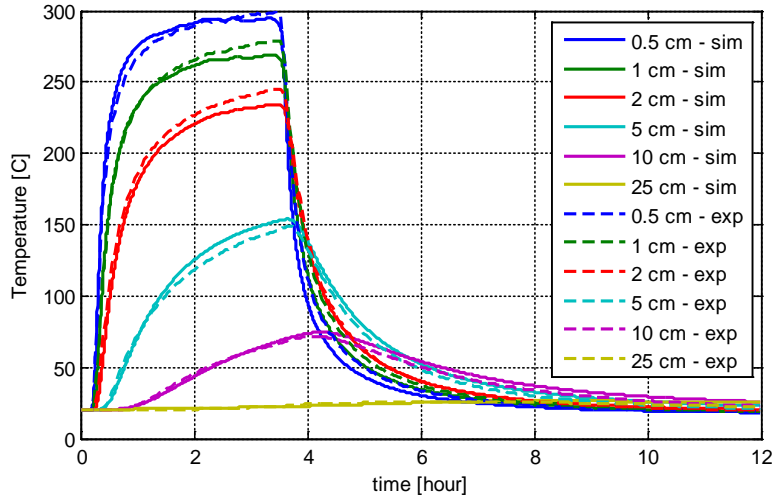


Figure 6 – simulation vs. laboratory heat experiment’s results for dry soil condition, including two assumption: Heat loss in the horizontal direction and linear change of the K with the temperature

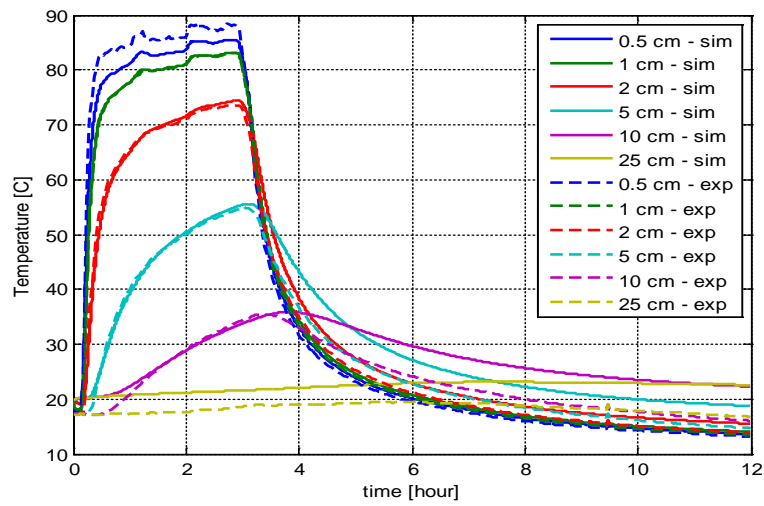


Figure 7 - simulation vs. laboratory heat experiment’s results including the heat loss assumption for the saturated soil condition